INSTITUTE OF PHYSICS PUBLISHING PHYSIOLOGICAL MEASUREMENT

Physiol. Meas. **23** (2002) 149–158 PII: S0967-3334(02)30765-2

Design and performance of the UCLH Mark 1b 64 channel electrical impedance tomography (EIT) system, optimized for imaging brain function

R J Yerworth[1], R H Bayford[1,2], G Cusick[3], M Conway[3] and D S Holder[1]

[1] Department of Clinical Neurophysiology, Middlesex Hospital, University College London, London W1T 3AA, UK
[2] School of Health, Environment and Biological Sciences, Middlesex University, Archway Campus, London N19 5ND, UK
[3] Department of Medical Physics and Bioengineering, Shropshire House, 11-20 Capper Street, University College London Hospitals NHS Trust, London WC1E 6JA, UK

Received 25 October 2001
Published 28 January 2002
Online at stacks.iop.org/PM/23/149

Abstract

The UCLH Mark 1b is a portable EIT system that can address up to 64 electrodes, which has been designed for imaging brain function with scalp electrodes. It employs a single impedance-measuring circuit and multiplexer so that electrode combinations may be addressed flexibly using software. It operates in the relatively low frequency band between 225 Hz and 77 kHz, as lower frequencies produce larger changes during brain activity, and has a videocassette-sized headbox on a lead 10 m long, connected to a base box the size of a video recorder, and notebook PC, so that recordings may be made in ambulant subjects.

Its performance was assessed using a resistor–capacitor network, and two saline-filled tanks—a cylindrical Perspex one and a latex one which contained a human skull. System signal-to-noise ratio was better than 50 dB and the maximum reciprocity error less than 10% for most frequencies. The CMMR was better than 80 dB at 38 kHz and a sponge, 20 mm across, which caused a local 12% impedance increase, was correctly localized in images. This suggests that the system has adequate performance to image impedance changes of 5–50% known to occur in the brain during normal activity, epilepsy or stroke; clinical trials to image these conditions are in progress.

Keywords: EIT, hardware, design, performance

1. Introduction

1.1. Requirements of an EIT system for imaging brain function

Since the advent of electrical impedance tomography (EIT), many groups have developed their own EIT systems (see Boone *et al* (1996) for a review), each group designing a system to meet the needs of their application.

Our group at University College London has focused on developing EIT to image brain function. This has several different requirements compared to systems designed for use elsewhere in the body (Holder *et al* 1994): (1) in order to maximize the sensitivity of EIT to brain impedance changes, the current injecting electrodes need to be diametrically opposed to each other across the head (Tarassenko *et al* 1985, Bayford *et al* 1996). Other EIT systems use adjacent electrodes to inject current or use optimized current patterns which utilize several electrodes. For 3D imaging of the brain, true diametric current injection cannot be used as the head cannot be approximated to a cylinder, unlike most other areas where multiple rings of electrodes have been used to achieve 3D imaging (Newell *et al* 2001). Thus any EIT system for 3D imaging of the head requires a flexible electrode protocol that can be completely controlled through software, to enable more complex protocols to be achieved and assessed during development and testing. (2) One of the principal intended uses is to record impedance changes during seizures in patients receiving a pre-surgical assessment for epilepsy surgery. These are admitted to a Telemetry ward for several days, and EEG recordings are made until several seizures are recorded. Measurements are made using a lead about 10 m long, so that subjects may move freely around their bed during the period of observation. Our system was therefore designed so that a small headbox could be worn by the patient, attached to a distant workstation by a lead 10–20 m long, so that the patient can move around near their bed. (3) The potential applications for EIT imaging of brain function include normal activity or neurological conditions such as stroke or epilepsy. The main principle by which changes occur in the brain with EIT at some tens of kHz is that the impedance is altered by changes in blood volume or by the occurrence of cell swelling. Cell swelling causes an increase in resistance because water moves from the extracellular to the intracellular space, and current at these frequencies is restricted to the extracellular space. Increased blood volume causes a decrease in resistance because blood has a lower resistivity than brain. Both these effects are larger at lower frequencies because applied current starts to cross the capacitative cell membranes at higher frequencies (see Holder 1994). On the other hand, recording at lower frequencies may result in poorer image quality, because electrode impedance is greater and may lead to instrumentation errors. Nevertheless, we have been able to obtain good images in saline-filled tanks at frequencies down to 1800 Hz (Holder *et al* 1999). We have therefore designed this system to be able to apply frequencies between 225 Hz and 80 kHz, a much lower band than other EIT systems, in order to give us flexibility in assessing which frequency gives optimal images in practice.

1.2. Description of the UCLH Mark 1b

This instrument is based on the 16 electrode UCH Mark 1a (Holder *et al* 1999) but has the capacity for 64 electrodes and several other improvements. It utilizes a single impedance-measuring circuit multiplexed up to 64 electrodes. Current is applied to two selected electrodes and voltage is recorded from another pair. Physically, the system is divided into two sections, a base box containing most of the electronics and a headbox approximately $19 \times 10 \times 4$ cm, which can be comfortably worn by the subject, containing the current source and cross point switches. The two boxes are separated by a ribbon cable up to 10 m in length, which allows

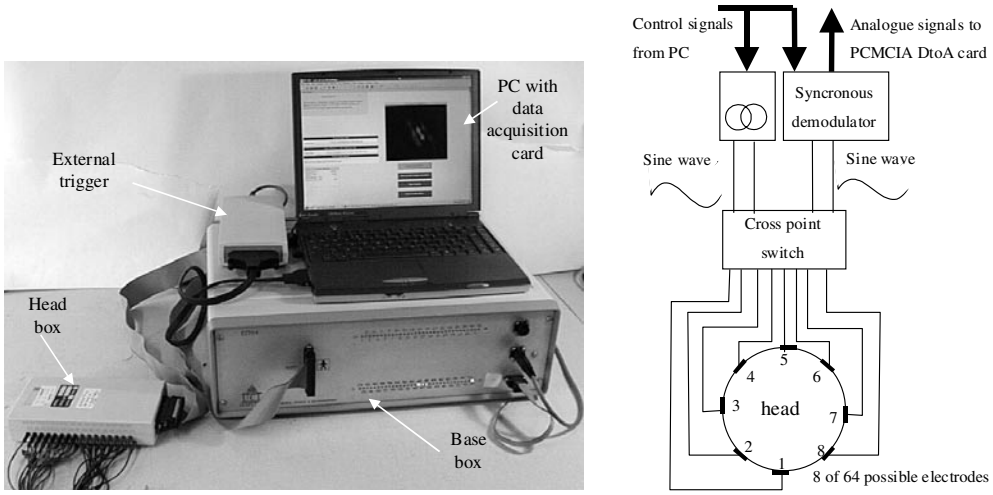

Figure 1. Photo and schematic diagram of UCH 1b.

freedom of movement to the subject. The recorded voltage is buffered in the head box and passed as an analogue signal to the base box, where it is demodulated. The demodulated signal is then passed as a higher-voltage analogue signal to a notebook PC, where the signal is digitized (figure 1).

The current source is based on a current conveyer voltage to current converter (CCII01) (Toumazou *et al* 1990). Its output impedance in the UCLH Mark 1b is 537 kΩ/28 pF. A synchronous-demodulation voltage sensing circuit, with differential input impedance of $>$150 kΩ at 38.4 kHz, yields the magnitude of the impedance. However, since signal phase is dependent on the relative positions of the sense and receive electrodes, as well as the characteristics of the object under test, a programmable phase shift is needed so that the demodulation occurs in-phase with the signal. This facility is included in the demodulation circuitry, enabling a different phase to be used for each electrode combination. Electrodes are selected using a set of cross point switches (MITEL MT8816), which enables any combination of drive and receive electrodes to be selected. The system operates at a single frequency, selectable from a range of 18 frequencies between 225 Hz and 77 kHz. Unscreened cables are used to reduce the weight and bulk of leads. This decision was taken at an early stage in its design, because relatively low frequencies are used, and it does not appear to degrade system performance appreciably. The system can take more than 600 measurements per second, which corresponds to about 3 images a second using 31 electrodes and 258 electrode combinations. The common mode performance of the system is enhanced by isolating the current source from the receive amplifier, which minimizes the effect of imbalance in the current source outputs (Cusick *et al* 1994).

Two features are provided to reduce system noise. On the current side, the output of the current conveyor has a frequency-dependent scaling resistor network as well as a software controllable current setting. These work together so that the current setting controls the proportion of the maximum permissible current (IEC601-1 for patient auxiliary current (100 μA rms max for frequencies less than 1 kHz, rising at 20 dB per decade up 1 mHz)) which is delivered, so that, for a given current setting, the injected current (mA) increases with frequency. Digitization noise on the receive side is minimized by use of a programmable gain amplifier so that the digitized voltage represents a sizeable proportion of the full range.

Optimal gain settings for each step of an electrode protocol can be downloaded to the system along with the electrode protocol and the phase information for the demodulation.

The system is designed to meet medical safety requirements under normal and single fault conditions. This is both with regards to leakage currents and the injected current (IEC601), the system having a current-sensing circuit which trips, cutting off current injection, if the system operator chooses too high a current setting for the chosen frequency. A medical grade power supply is used for powering both the system and the laptop PC.

Software control of the system is provided through a graphical user interface on a laptop computer which connects to the system via a RS232 Serial port and allows the user to select the electrode protocol, current setting, experiment duration and repetition rate. It also provides automatic gain and phase optimization as these are best recalculated for each subject. Image data are passed from the system to the computer using a 12 bit analogue to digital PCMCIA card.

1.3. Purpose and rationale of measurements

This paper summarizes key parameters of the system design and presents an objective assessment of its performance.

Three indirect measures of performance were recorded—common mode rejection ratio, reciprocity and noise. These were calculated as follows:

Common mode rejection ratio (CMRR) is defined as (Brown *et al* 1999)

$$20 \times \log(\text{signal gain/common mode gain}). \tag{1}$$

The common mode gain may be measured by tying together the two inputs of the differential amplifier under investigation and injecting a known signal. An imbalance (usually 1 kΩ) may be inserted to test the tolerance of the system to mismatches in lead resistance.

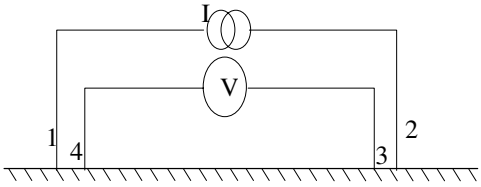

Figure 2. Electrode measurement set-up.

Reciprocity error—EIT impedance measurements are normally obtained using a four-point probe set-up (see figure 2). This is to remove the effects of electrode/skin interface impedance from the measurements. In a perfect system, the voltage measured between electrodes 1 and 2 when current is injected between electrodes 3 and 4 will be identical to the measurement shown in figure 2. However, in reality, imbalances in the resistance and capacitance of the different electrode leads, electrode/skin interfaces, multiplexer paths, etc will result in there being a difference between these two measurements.

Reciprocity error is defined as

$$((V_\mathrm{n} - V_\mathrm{r})/V_\mathrm{n}) \times 100\% \tag{2}$$

where V_n and V_r are the voltages recorded in the 'normal' and 'reverse' senses.

Noise–system noise, is a measure of signal reproducibility and may have many causes, the three main ones being: current drive random noise, measurement amplifier random noise and

transimpedance fluctuations which are dominated by physiological signals and noise (Meeson *et al* 1996). Noise in this situation was assessed according to the Sheffield group (Wilson *et al* 1991): the signal-to-noise measurement (SNR) for an EIT system was defined as the ratio of the mean and standard deviation for a contiguous sequence of measurements and expressed in dB.

In addition to the above measurements, images of the relatively small impedance changes due to a sponge were recorded in a saline-filled tank. The changes due to the sponge (12% locally) were similar in magnitude to those during conditions like epilepsy or evoked activity, and so were a reasonable test of the overall function of the system.

2. Method

2.1. The Cardiff –Cole phantom

The Cardiff–Cole phantom (Griffiths 1995) was used because it is well documented and stable with respect to temperature and time. It is a resistor–capacitor wheel phantom designed to simulate a cylinder of homogeneous conductor with complex impedance, Z^*, obeying the Cole equation. The phantom was originally designed for use with 16 drive and 16 receive electrodes interleaved. Built into the phantom are three rings of jumpers. The first two sets of jumpers (J1 & J2) allow four different sets of spectroscopic parameters, specified in terms of characteristic frequency (f_c), and the ratio of the limiting values of resistance at high and low frequencies (R_0/R_∞). The third of these (J3) short out simulated electrode impedances which are identical for each electrode.

With J3s removed the transfer impedance of the phantom varies between 330 Ω at 38.4 kHz and 1500 Ω at 4800 Hz.

2.2. Common mode rejection

The circuit shown in figure 3 was used to obtain CMRR measurements. A 1 kΩ resister was used to provide a constant common mode input voltage. Since the system uses a floating current source, the current source and voltage measurement circuit ground planes were connected together for this measurement. V_1 was the common mode input voltage, measured with the system's sense amplifier at a low gain setting of 10. Then the amplifier gain was increased to 8000 (max) and its inputs were connected together and to the same point on the phantom where the common mode voltage was measured. The output voltage V_2 of the amplifier was measured. A current setting in the range 0.4–3 mA, depending on frequency, was used for both measurements. CMMR was calculated according to equation (1) where

$$\text{common mode gain} = (V_2 \times 10)/V_1 \tag{3}$$

and the signal gain is taken as 8000.

The experiment was repeated with a 1 kΩ resister (approximately twice the transfer impedance of the head at 38.4 k) in series with electrode 3. In this case gains of 4 (V_1) and 400 (V_2) were used in order to prevent saturation of the signal.

2.3. Reciprocity errors

200 frames of image data were obtained from the Cardiff phantom (J3s removed, enabling simulated electrode impedances as in section (2.1)), using a current setting of 0.1–0.4 mA and gain of 100 for all frequencies. Data from all the image frames were averaged and then the

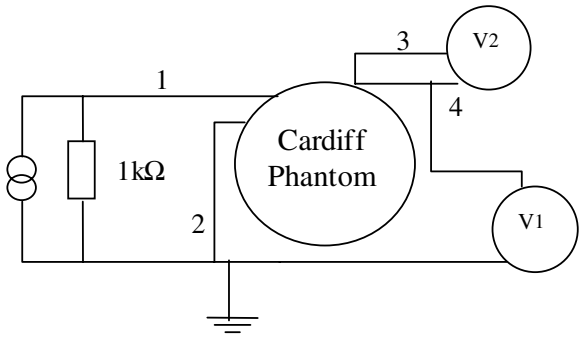

Figure 3. Circuit diagram for CMRR measurement.

reciprocity for each electrode combination was calculated for each frequency. The figure cited below is the largest error from any electrode combination—'peak reciprocity error'.

2.4. Signal-to-noise ratio

The ratio of the mean and standard deviations was calculated for 200 images of continuous data from a cylindrical Perspex tank, diameter 88 mm, height 50 mm, holding 300 ml of 0.2% saline, which had a single ring of equally spaced stainless steel electrodes, each 10 mm in diameter. A current of 0.1–0.4 mA and gain of 100 were used for all frequencies (4.8–77 kHz).

2.5. Response to a uniform impedance change

A uniform change in the impedance of a uniform phantom should cause an equal proportionate change in all voltage measurements. Imbalances between the different measurement channels will introduce errors and were assessed by assessing the radial symmetry of recorded voltages.

A cylindrical tank, diameter 88 mm, height 50 mm, holding 300 ml of fluid was initially filled with 0.2% saline. Eight measurement electrodes were attached, equally spaced about a plane half-way up the tank. The ground electrode was attached equidistant between electrodes eight and one. At one-minute intervals during continuous data collection 3 ml of saline was removed from the tank, replaced with 3 ml of distilled water and the fluid mixed with a syringe. Five such dilutions were performed;; each time 1% of the fluid was exchanged which, at these concentrations, corresponds approximately to a 1% impedance increase.

Data were normalized with respect to the first minute of data acquisition. For each 30 s period after the system had stabilized following saline dilution, the mean (M_{ec}) of the percentage change from baseline, was found for each electrode combination. These results were combined to give the mean (mean(M_{ec})) for all electrode combinations, with the corresponding standard deviation (sdv(M_{ec})) to indicate the variance between electrode combinations.

2.6. Qualitative image quality

A head-shaped latex tank containing a human skull was employed. A gap of 5 mm existed outside the outer skull surface to simulate the scalp. Both the cranium and outer space were filled with 0.2% saline, and recordings were made using 32 chlorided silver discs, each 10 mm in diameter, set at roughly equal spacing into the latex (Tidswell *et al* 2001). Images

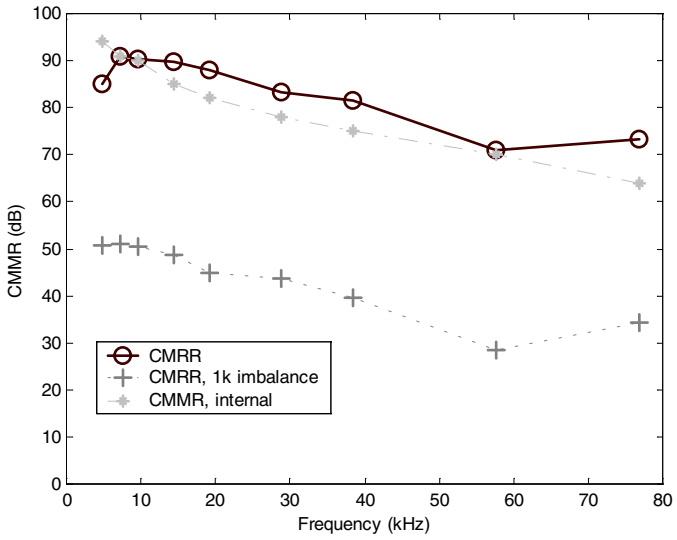

Figure 4. CMMR of UCLH 1b.

were produced of the difference with saline alone and after the introduction of a cylindrical polyurethane sponge (density 5% w/v, 2.0 cm diameter, 2.5 cm length, Vitafoam, UK), representing a 12% impedance change (Tidswell *et al* 2001), through the foramen magnum.

The image was reconstructed from the impedance changes by multiplication with an inverted sensitivity matrix calculated from an analytical model of a homogeneous sphere (Gibson 2000).

3. Results

3.1. CMRR

At low frequencies (<20 kHz), the CMRR was 90 dB and fell to 70 dB at high frequencies (>50 kHz). These were within 5 dB of the values recorded from the amplifier alone ('CMMR internal', figure 4), except for the lowest and highest frequencies. Addition of the 1 kΩ imbalance reduced the CMRR at all frequencies by approximately 40 dB.

3.2. Reciprocity

The peak reciprocity error of the system (figure 5(a)) was least over the mid-frequency range of 10–40 kHz, with a maximum error of <2% for most frequencies;; errors increased at both extremes.

3.3. Signal-to-noise ratio

As with reciprocity, the system performed best in its mid-frequency range (10–30 kHz) with mean SNR levels of >50 dB (figure 5(b)). The SNR was slightly worse at the highest (76.8 kHz) and lowest (4.8 kHz) but still better than 30 dB.

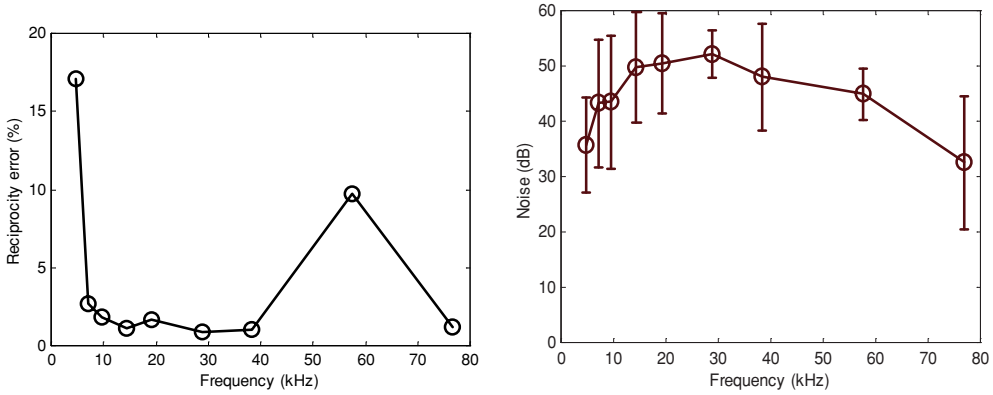

(a) (b)

Figure 5. (a) Maximum reciprocity error as a function of frequency. (b) Mean noise as a function of frequency (error bars ±STD).

Table 1. Means (mean(M_{ec})) and standard deviations (sdv(M_{ec})) of impedance changes recorded for a uniform impedance change.

No. dilutions	mean(M_{ec}) (% change)	sdv(M_{ec}) (% change)
0	0.00	0.00
1	1.12	0.26
2	2.14	0.24
3	3.30	0.16
4	4.44	0.21
5	5.64	0.25

3.4. Response to uniform impedance change

Impedance increased linearly with a uniform impedance change (table 1). The gradient was 1.11 with r^2 value of 0.999 over the range of 5% change measured. This indicates the change is highly linear. The SD of inter-electrode differences were less than 0.26%.

3.5. Qualitative image quality

An impedance increase is clearly seen in the first three slices, at the 6 o'clock position, which corresponded to the true position of the sponge in all three dimensions (see figure 6).

3.6. Discussion

This system specification meets the criteria for human brain imaging with regards to safety, electrode protocol, frequency range and physical size. The common mode performance measured is acceptable for a multiplexed system and is comparable to other designs (Boone *et al* 1996, table 6). It is likely to be an underestimation of the system's performance because ground separation between current source and sense circuit, designed to reduce the common mode signal, was removed for the purpose of this measurement. The reciprocity errors recorded here are slightly better than those reported for the Sheffield Mk3.5 (Brown *et al* 2001) although this may be because they have reported results from clinical data. System

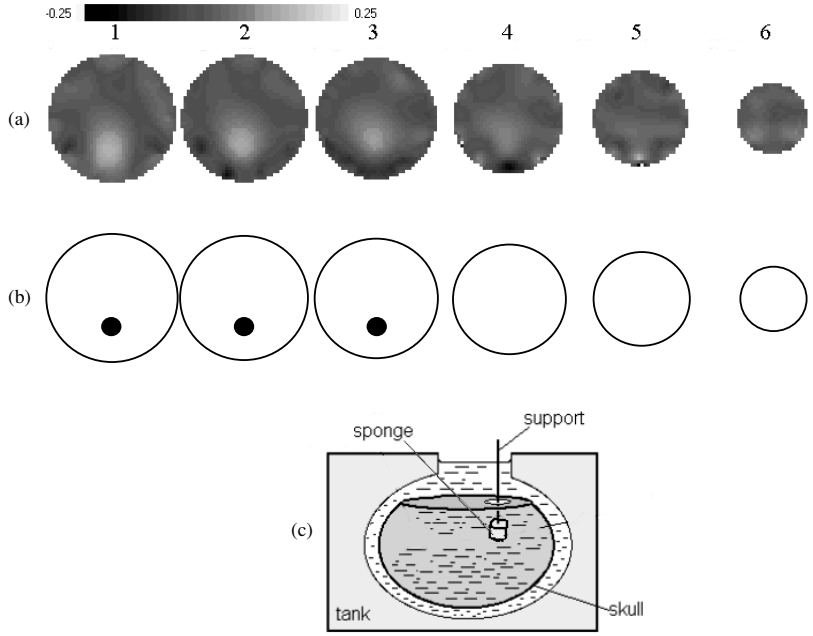

Figure 6. (a) Image (six horizontal slices), (b) expected position and (c) schematic of sponge in realistic head-shaped tank with human skull.

noise is also comparable with the 40 dB noise reported for the Sheffield Mk3.5 (Wilson *et al* 2001) although the UCLH shows greater frequency dependence. The UCLH Mark 1b is able to detect a localized 12% impedance change within a skull. These measurements of system performance indicate that the system should be able to image blood volume changes in the human brain using scalp electrodes.

The system represents a compromise between practicality for its intended use, cost and electronic performance. A major cause of error in EIT is common mode error, and this may be minimized by avoiding the use of a multiplexer, as with the Sheffield Mark 3.5 system (Wilson *et al* 2001). We have elected to use a multiplexer in order to retain flexibility in addressing electrodes, facilitating experimentation with differing approaches to reconstruction. We also elected to use unscreened leads on the grounds of simplicity and reduction of bulk in electrode leads, which is a significant issue if 64 leads are to be applied to the head. In this application, lower frequencies are optimal for imaging brain function, at least at a single applied frequency, and so it appears that these compromises were indeed acceptable, as stray capacitance is less of a problem. The ultimate test is whether the system can produce acceptable images—this appears to be the case, since it was possible to obtain good images of the low impedance contrast produced by a sponge, in a realistic head-shaped tank, even with the use of a reconstruction algorithm which did not model the true geometry of the head. No adverse effects due to the use of unscreened leads were observed in any of the experiments described in this paper, despite the presence of other electrical equipment nearby.

This system is currently being used in clinical trials of EIT during epilepsy and evoked potentials. It represents the culmination of a decade of effort. At present, it is being used with the simplified reconstruction algorithm (Gibson 2000) but will shortly be used with one

based on a finite element model of the true geometry of the head. This should give the best possibility of producing clinically useful images of brain function. Future work will be to assess its use in these and similar conditions, such as stroke and head injury, together with realistic 3D algorithms which incorporate further prior information such as anisotropy, and the development of a similar hardware system which will permit multifrequency imaging up to 1 MHz.

References

Bayford R H, Boone K G, Hanquan Y and Holder D S 1996 Improvement of the positional accuracy of EIT images of the head using a language multiplier reconstruction algorithm with diametric excitation *Physiol. Meas.* **17** (suppl) A49-A57

Boone K G and Holder D S 1996 Current approaches to analogue instrumentation design in electrical impedance tomography *Physiol. Meas.* **17** 229–47

Brown B H, Primhak R A, Jackson M J, Milnes P and Smallwood R H 2001 Neonatal lung imaging using an 8 electrode EIT system *Biomedical Applications of EIT (London)*

Brown B H, Smallwood R H, Barber D C, Lawford P V and Hose D R 1999 *Medical Physics and Biomedical Engineering* (Bristol: Institute of Physics Publishing)

Cusick G, Holder D S, Birkett A and Boone k 1994 A system for impedance imaging of epilepsy in ambulatory human subjects *Innov. Technol. Biol. Med.* **15** 40–6

Gibson A 2000 *Electrical Impedance Tomography of Human Brain Function* (London: University College London)

Griffiths H 1995 A Cole phantom for EIT *Physiol. Meas.* **16** (suppl) A29–A38

Holder D S, Boone K and Cusick G 1994 Specification for an electrical impedance tomogram for imaging epilepsy in ambulatory subjects *Innov. Technol. Biol. Med.* **15** 33–9

Holder D S *et al* 1999 Assessment and calibration of a low frequency system for electrical impedance tomography (EIT), optimized for use in imaging brain function in ambulant human subjects *Ann. New York Acad. Sci. Proc. NYAS* **873** 512–9

Meeson S, Blott B H and Killingback A L T 1996 EIT data noise evaluation in the clinical environment *Physiol. Meas.* **17** (suppl) A33–A38

Newell J C, Blue R S, Isaacson D, Saulnier G J and Ross A S 2001 Phasic three-dimensional impedance imaging of cardiac activity *Biomedical Applications of EIT (London)*

Tarassenko L, Pidcock M, Murphy D and Rolfe P 1985 The development of impedance imaging techniques for use in the newborn at risk of intra-ventricular haemorrhage *IEEE Int. Conf. Electr. Magn. Fields Med. Biol.*

Tidswell A T, Gibson A, Bayford R H and Holder D S 2001 Validation of a 3D reconstruction algorithm for EIT of human brain function in a realistic head-shaped tank *Physiol. Meas.* **22** 177–85

Toumazou C, Lidgey F J and Haigh D G 1990 Analogue IC Design: the Current-Mode Approach *(IEE Circuits and Systems Series 2)* (Peter Peregrinus)

Wilson A J, Milnes P, Waterworth A R, Smallwood R H and Brown B H 2001 Mk3.5: a modular multi-frequency successor to the Mk3a EIS/EIT system. *Physiol. Meas.* **22** 49–54